ROYAL SOCIETY
OF CHEMISTRY

## PAPER

# π-Conjugated gradient copolymers suppress phase separation and improve stability in bulk heterojunction solar cells†

Edmund F. Palermo,[a] Seth B. Darling[bc] and Anne J. McNeil*[a]

Gradient sequence copolymers of 3-hexylthiophene (90 mol%) and 3-(6-bromohexyl)thiophene (10 mol%) were synthesized by catalyst transfer polycondensation. Post-polymerization conversion of the side-chain bromides into azides and subsequent Cu-catalyzed azide–alkyne cycloaddition installed $C_{60}$-functional groups. Comparing blends of poly(3-hexylthiophene) (P3HT) and phenyl-C61-butyric acid methyl ester (PCBM) with and without the gradient copolymer additive revealed that, when the gradient copolymer was present, micron-scale phase separation was not observed even after prolonged thermal annealing times. In addition, the PCBM was still able to quench the P3HT emission after thermal annealing, indicating that the donor–acceptor interfacial area is maintained. Together, these data suggest that the gradient copolymers are an effective compatibilizer for P3HT/PCBM physical blends. This stabilized film morphology led to stable power conversion efficiencies (PCE) of the corresponding bulk heterojunction solar cells even upon extended thermal annealing. Nevertheless, the short circuit current and fill factor were reduced when the gradient copolymer was present, leading to a lower PCE. Overall, these gradient copolymer additives represent a promising tool for inhibiting micron-scale phase separation and producing robust polymer/fullerene-based solar cells.

## Introduction

Due to a unique combination of semiconducting properties with mechanical flexibility, organic π-conjugated small molecules and polymers are being utilized as the active layers in solar cells.[1] One of the most extensively studied systems is the physical blend of poly(3-hexylthiophene) (P3HT, the electron donor) and phenyl-C61-butyric acid methyl ester (PCBM, the electron acceptor).[2] In these bulk heterojunction (BHJ) devices, the two materials initially undergo nanoscale phase separation during solution processing, and this phase separation is further evolved through solvent vapor or thermal annealing.[3,4] This nanoscale morphology provides extensive donor–acceptor interfaces, which promote exciton dissociation. Upon extended aging or thermal annealing, however, phase separation continues, generating micron-scale domains, which dramatically reduces the interfacial area and thus reduces charge

dissociation efficiency. As a consequence, the long-term stability and performance of the solar cell is compromised.[3,4]

Stabilizing physical blends of organic materials has been extensively studied and to some extent, solved for amorphous homopolymers. Although chemically dissimilar homopolymers naturally undergo phase separation in physical blends because the enthalpic penalty for mixing outweighs the entropic gains,[5] additives that localize at the interface can stabilize blends against this phase separation. For example, Torkelson and co-workers have demonstrated that gradient copolymers, which exhibit a gradual change in composition along the normalized chain length, localize at the interfaces in physical blends of the two corresponding homopolymers.[6,7] As a consequence, these additives broaden the interfacial width, lower the interfacial tension and suppress phase separation. Block copolymers have also been used as additives to reduce phase separation in polymer blends,[8] but are ultimately limited by their tendency to form micelles.[6,7] Because gradient copolymers resist micelle formation until reaching concentrations ten-fold greater than their block copolymer counterparts,[9] gradient copolymers may be a promising approach for compatibilizing polymer/fullerene blends.[10,11]
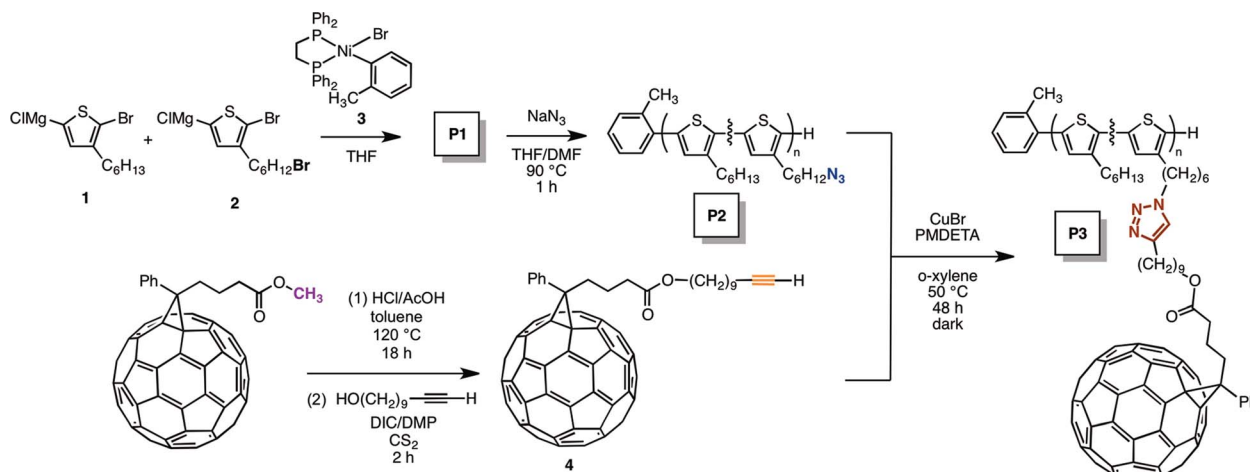
Using catalyst transfer polycondensation (CTP)[12] we synthesized a gradient copolymer containing P3HT and PCBM wherein the side chain composition gradually varies from one chain end to the other (Scheme 1).[13] The side chains varied from $C_6H_{13}$ to $C_6H_{12}Br$. We then converted the Br moieties to a PCBM

*[a]Department of Chemistry and Macromolecular Science and Engineering Program, University of Michigan, 930 North University Avenue, Ann Arbor, MI 48109-1055, USA. E-mail: ajmcneil@umich.edu*

*[b]Center for Nanoscale Materials, Argonne National Laboratory, 9700 S. Cass Avenue, Argonne, IL 60439, USA*

*[c]Institute for Molecular Engineering, The University of Chicago, Chicago, Illinois 60637, USA*

† Electronic supplementary information (ESI) available: Materials and methods, synthetic procedures, characterization data, and device fabrication. See DOI: 10.1039/c3tc32512a

Scheme 1

derivative to access the targeted donor/acceptor gradient copolymer architecture. The impact of these materials on the phase separation, photoluminescence, and current–voltage characteristics of P3HT/PCBM devices is demonstrated. The gradient copolymer was found to compatibilize the P3HT/PCBM blend and enhance the thermal stability. We conclude that gradient copolymer additives represent an effective tool for inhibiting micron-scale phase separation in physical blends of polymers with fullerenes, which can lead to improved long-term stability of the solar cell.

## Experimental

Detailed experimental procedures and full characterization data can be found in the ESI.†

## Results and discussion

### Polymer synthesis

The gradient copolymers described herein were prepared using a living, chain-growth polymerization method known as catalyst transfer polycondensation.[12] Depending on the (co)monomer and catalyst structures, the CTP method can afford materials with defined molecular weights (MW), low dispersities ($Đ$), high regioregularities (RR), and specific end groups. Herein, a gradient copolymer composed of 3-hexylthiophene (3HT, 90 mol%) and 3-(1-bromohexylthiophene) (3BrHT, 10 mol%) was prepared according to our previously reported procedure (Scheme 1 and ESI†).[13a] The key to obtaining a gradient copolymer is the gradual, syringe pump addition of monomer **2** to a solution containing both monomer **1** and catalyst **3**. ^{1}H NMR spectroscopic analysis of the aliquots withdrawn during the polymerization showed that the copolymer composition varied linearly with normalized chain length (as determined by gel permeation chromatography (GPC)), confirming a gradient sequence. (See Fig. 1 for a comparison of the gradient sequence distribution relative to the analogous random and block copolymer with the same composition.) The obtained gradient
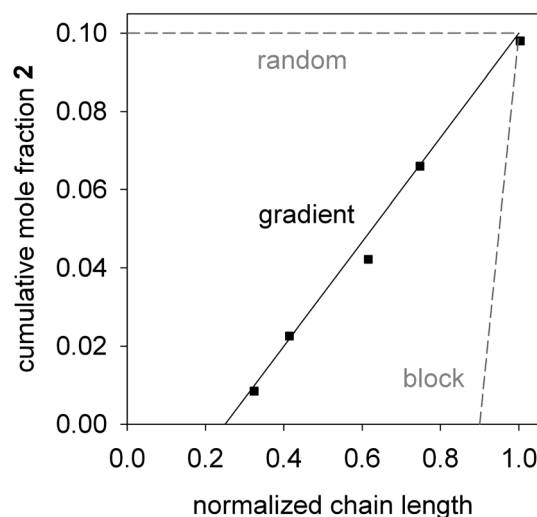


**Fig. 1** Plot of the cumulative mole fraction of 3BrHT in the copolymer as a function of the normalized chain length.

copolymer (**P1**) exhibited a number-average molecular weight ($M_n$ = 23 kDa) in agreement with the theoretical value (18 kDa), narrow MW dispersity ($Đ$ = 1.17), and high regioregularity (>99%) (Fig. 2). The cumulative mole fraction of the 3BrHT comonomer was 0.10 at the end of the polymerization, which matched the feed composition. Attempts at higher mol% incorporation led to extensive cross-linking during the subsequent functionalization reactions, as described in detail below. Nevertheless, 10 mol% of 3BrHT corresponds to 35 wt% PCBM in the final copolymer, which is within the range of typical compositions of BHJ solar cells.[2]

Two post-polymerization functionalization reactions were utilized to convert the P3HT/P3BrHT gradient copolymer (**P1**) into the target fullerene-functionalized copolymer (**P3**) (Scheme 1). The side-chain bromides were first converted to azides using NaN$_3$.[14] ^{1}H NMR spectroscopic analysis confirmed quantitative conversion to the azides (Fig. 2). As expected, the resulting copolymer (**P2**) showed little change in its GPC profile
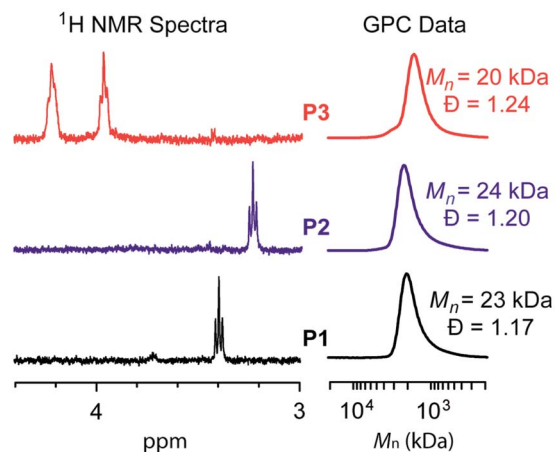
**3402** | *J. Mater. Chem. C*, 2014, **2**, 3401–3406

This journal is © The Royal Society of Chemistry 2014

Fig. 2 (Left) Selected regions of the $^1$H NMR spectra for polymers **P1** (pendant bromide), **P2** (pendant azide), and **P3** (pendant fullerene derivative) showing complete conversion at each synthetic step. (Right) Gel permeation chromatography data for polymers **P1**, **P2**, and **P3** after each synthetic transformation.

after the post-polymerization reaction (Fig. 2). In a separate step, the methyl ester of commercial PCBM was converted to the corresponding alkynyl ester (**4**) *via* hydrolysis and esterification using undec-10-yn-1-ol.

Azide-functionalized gradient copolymer **P2** was then reacted with **4** using copper-catalyzed azide–alkyne cycloaddition (CuAAC) to obtain **P3**. This reaction required some optimization to avoid extensive polymer cross-linking. The recommendations of Hashimoto and co-workers[15] that were necessary included keeping the reaction mixture strictly air-free, rigorously purifying the solvent and ligand, and using an excess of **4**. In addition, we found that a longer linker between the alkyne and fullerene lowered the prevalence of cross-linking and afforded materials with higher solubility. Using these optimized conditions, minimal broadening of the molecular weight distribution was observed by GPC ($Đ = 1.24$)[16] and $^1$H NMR spectroscopic analysis confirmed the complete conversion of the side chain azides to triazoles (Fig. 2). As mentioned earlier, attempts to functionalize copolymers with higher mol% 3BrHT were unsuccessful due to polymer cross-linking (ESI†). With successful preparation of gradient copolymer **P3**, we proceeded to measure the impact of this additive on physical blends of P3HT and PCBM.

### Suppressed phase separation

One of the prevailing hypotheses about the decrease in power conversion efficiencies upon prolonged thermal annealing for P3HT/PCBM-based solar cells is that the materials undergo micron-scale phase separation, which reduces both the interfacial area and the charge dissociation efficiency.[3,4,17] We confirmed the formation of needle-shaped PCBM aggregates (~5–30 μm in length and ~1 μm in width) in the conventional P3HT/PCBM blend after thermal annealing (150 °C for 1 h, Fig. 3A). Based on literature precedent,[6,7] we hypothesized that gradient copolymer additives might suppress this phase
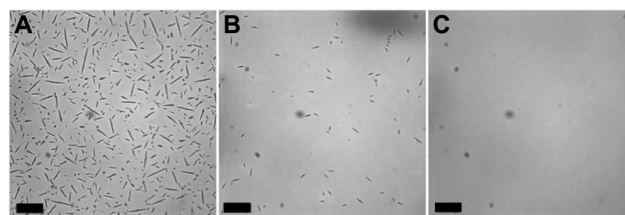


Fig. 3 Optical microscope images of a P3HT/PCBM blend after annealing at 150 °C for 1 h with (A) 0 wt%, (B) 1 wt% and (C) 10 wt% gradient copolymer additive (**P3**). The scale bar represents 25 μm.

separation. Indeed, when the gradient copolymer was included in the blend at 1 wt%, the size and density of PCBM needle-shaped aggregates was markedly reduced (Fig. 3B). When 10 wt% gradient copolymer was included, no evidence of micron-scale phase separation was observed (Fig. 3C). These results are consistent with the notion that the gradient copolymer serves as a compatibilizer for the blend. In principle, this thermal stability should translate to increased longevity in the bulk heterojunction-based solar cell (*vide infra*).

### Photoluminescence quenching

To provide further evidence that the gradient copolymer additive is an effective tool to inhibit phase separation, we measured the steady-state photoluminescence (PL) intensity of P3HT films and compared it to the P3HT/PCBM blends with and without gradient copolymer additive. Contour maps were generated to describe the thin film PL intensity as a function of the excitation and emission wavelengths (Fig. 4). As expected, the PL intensity map for the pristine P3HT film were similar after annealing for 10 min *versus* 60 min at 150 °C (Fig. 4A and B). In contrast, the P3HT/PCBM blend initially showed significant PL intensity quenching due to efficient charge transfer from the donor P3HT to the acceptor PCBM (Fig. 4C).[18] This result suggests that these two materials are intimately mixed at the nanoscale, which enables efficient charge transfer at the interface. Upon prolonged thermal annealing of this blend, however, the relative PL intensity increased (Fig. 4D). This decrease in quenching efficiency by PCBM is presumably due to the micron-scale phase separation that we observed in the optical microscope, which will create regions of phase-pure P3HT that are larger than the exciton diffusion limit. As a consequence, those excitons can be emissive, leading to enhanced PL intensity.

The blend containing P3HT/PCBM and 10 wt% gradient copolymer additive exhibited marked PL quenching even after prolonged thermal annealing (Fig. 4E and F). This result, in combination with the optical characterization data, strongly suggests that gradient copolymers are effective compatibilizers for the P3HT/PCBM blend. Based on these data, we anticipated that gradient copolymer additives would improve the thermal stability of the corresponding bulk heterojunction solar cells.

### Bulk heterojunction device performance

Photovoltaic devices were prepared with P3HT/PCBM with or without gradient copolymer additive as the active layer. The

This journal is © The Royal Society of Chemistry 2014

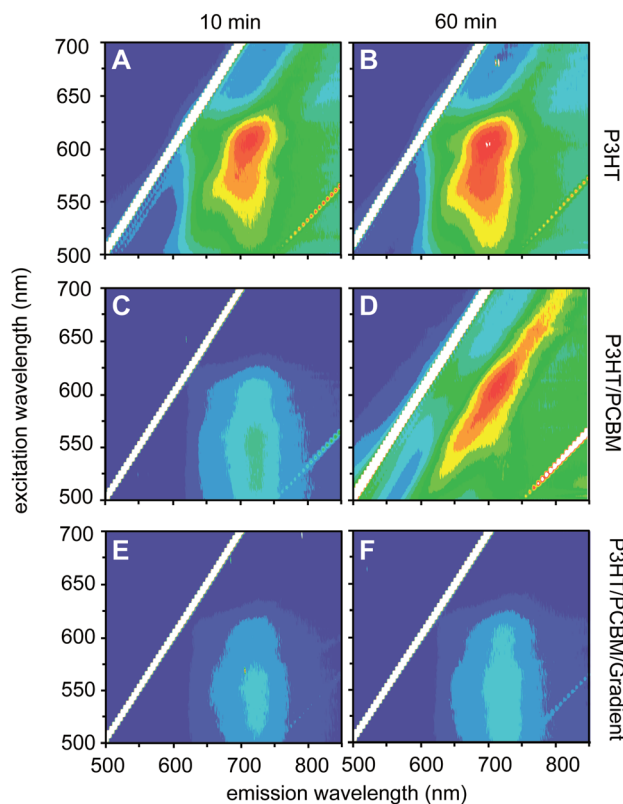*J. Mater. Chem. C*, 2014, **2**, 3401–3406 | **3403**

Fig. 4 Contour maps of PL intensity as a function of the emission and excitation wavelengths for (A and B) P3HT; (C and D) P3HT/PCBM; (E and F) P3HT/PCBM + 10 wt% gradient copolymer (P3). Each film was annealed at 150 °C for either 10 min (A, C and E) or 60 min (B, D and F). The color represents the relative PL intensity with red as the maximum.



Fig. 5 Current–voltage data for P3HT/PCBM blends with 0 wt% (black solid line), 1 wt% (blue dash-dot line), or 10 wt% (red dashed line) gradient copolymer additive (P3). The plots correspond to the devices (A) as cast and after annealing at 150 °C for (B) 10 min, (C) 30 min and (D) 60 min. The active area was 0.049 $cm^3$.

device architecture was glass/ITO/PEDOT:PSS/active layer/Ca/Al. Detailed descriptions of the fabrication procedure and overall device configuration can be found in the ESI.† To obtain statistically significant results, each thin film composition was tested twice on different regions of the same sample (to account for variation within a sample) and three unique samples of each composition were prepared and tested, giving a total of six measurements.

The conventional devices comprised of a P3HT/PCBM active layer without any copolymer additive showed typical current–voltage characteristics that improved after brief (10 min) thermal annealing (Fig. 5 A and B). Annealing for longer time, however, diminished the short circuit current density ($J_{sc}$) and resulted in lower overall PCE (Fig. 5C and D). The most straightforward explanation is that the charge dissociation efficiency has been reduced due to the changes in the donor/acceptor interfaces during phase separation. This conclusion is supported by the observed PCBM crystallite formation with a concomitant decrease in PL quenching.

In contrast, the blend of P3HT/PCBM with 10 wt% gradient copolymer additive showed dramatically different current–voltage data (Fig. 5). The observed "S-shaped" curves are often ascribed to charge build-up in the device, which opposes the flow of electrons from the anode to the cathode. There are several possib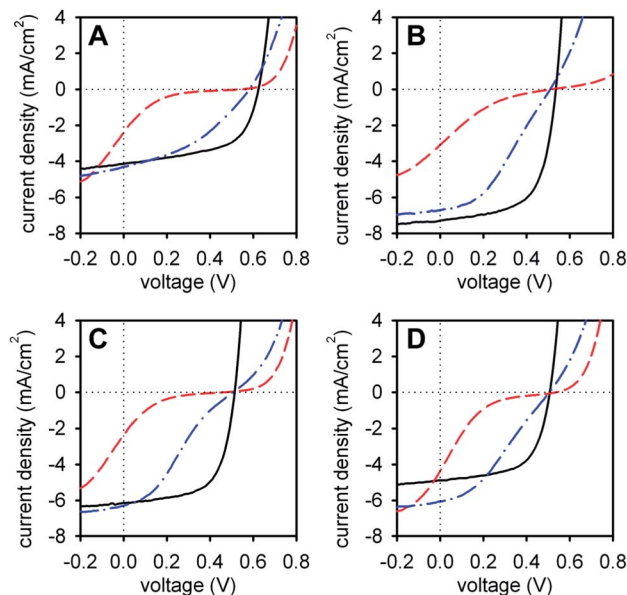le reasons for this behavior, including restricted recombination at the electrodes, blocking of the interfacial buffer layers, accumulation of charge-trapped states, or imbalance of the relative electron and hole mobilities in the active layer.[19] Although the gradient copolymers prevent micron-scale phase separation, they may also inhibit the growth of pure P3HT fibrils, which would restrict hole transport and, as a result, increase the likelihood of non-geminate recombination.[20] Indeed, the P3HT/PCBM blend exhibited some modest changes in the solid-state organization, as evidenced by powder X-ray diffraction and differential scanning calorimetry, when the gradient copolymer was added (ESI†). The origin of the $J$–$V$ curve distortion is outside the scope of this work, but will be a focus of our future efforts. Excitingly, the blend of P3HT/PCBM with 1 wt% gradient copolymer additive exhibited an improved $J$–$V$ curve shape relative to the sample with 10 wt% gradient, and also maintained superior thermal stability relative to the conventional devices.

Plots of the PCE, fill factor (FF), open circuit voltage ($V_{oc}$), and short circuit current density ($J_{sc}$) versus annealing time for all samples are highlighted in Fig. 6. While the 10 wt% gradient copolymer additive effectively suppressed phase separation in the blends, it also significantly reduced the device efficiency. On the other hand, using 1 wt% gradient copolymer led to reasonably improved PCEs relative to the devices containing 10 wt% gradient, while still maintaining the enhanced thermal stability. For comparison, the blends without gradient copolymer resulted in decreasing PCEs after annealing for longer than 10 min. When the loading was further reduced to 0.1 wt% gradient copolymer, the devices performed similarly to the blends without gradient copolymer (ESI†). Hence, it appears that the lower limit for device stabilization is between 0.1 and 1
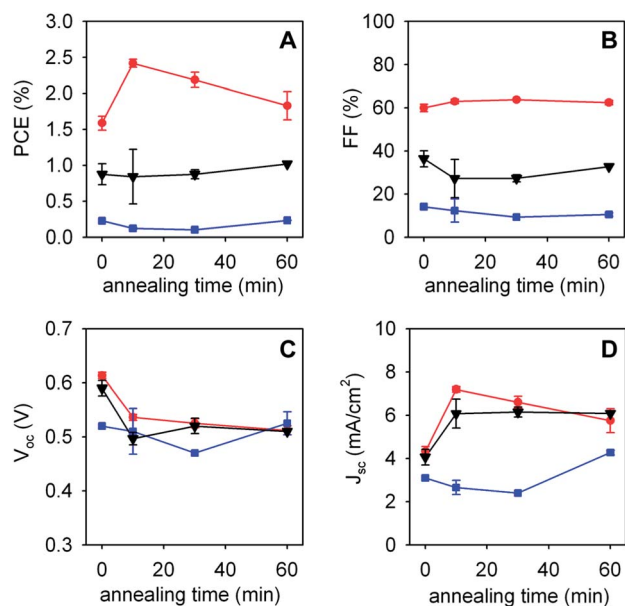
3404 | J. Mater. Chem. C, 2014, 2, 3401–3406

This journal is © The Royal Society of Chemistry 2014

**Fig. 6** Plots of the (A) power conversion efficiency (PCE), (B) fill factor (FF), (C) open circuit voltage ($V_{oc}$), and (D) short circuit current density ($J_{sc}$) as a function of annealing time for P3HT/PCBM blends with 0 (red circles), 1 (black triangles), and 10 (blue squares) wt% gradient copolymer additive (**P3**).

wt% gradient copolymer. This range is comparable to other processing additives used in organic solar cells, such as diiodooctane and octanedithiol.[21]

Overall, these results provide strong evidence that gradient copolymers can effectively stabilize the morphology of bulk heterojunction active layers and enhance their thermal stability, albeit with a reduced PCE. As such, these gradient copolymers are comparable (and in some cases, better) than other copolymer additives containing pendant fullerenes.[22] For example, both Jo and co-workers[23a] and Hadziioannou and co-workers[23b] reported modest improvements in thermal stability with a fullerene-containing copolymer additive, however the PCEs decreased over prolonged annealing times. In contrast, Fréchet and co-workers demonstrated that a non-conjugated block copolymer additive containing both P3HT and PCBM in the side-chains exhibited enhanced thermal stability even after extended annealing times with PCE ~2.5 wt%.[23c] Although the results reported herein are promising, the impact of gradient copolymer composition, sequence distribution, and molecular weight on P3HT/PCBM blend thermal stability and PCE represent areas for future exploration.

## Conclusions

Herein, a novel gradient sequence π-conjugated copolymer with pendant fullerenes was prepared and its impact on P3HT/PCBM blends was examined. We demonstrated that gradient copolymer additives represent a promising approach toward devices with long-term thermal stabilities. The obtained gradient copolymer inhibited micron-scale phase separation in P3HT/PCBM blends. As a consequence, these materials afforded

improved thermal stability in the corresponding bulk heterojunction solar cells. Nevertheless, the power conversion efficiency was reduced when the gradient copolymer was present, and this result was attributed to a reduction in phase-pure P3HT fibrils, which would hinder hole transport.

Future efforts will therefore focus on improving the device performance. Specifically, we will identify the ideal gradient copolymer structure by varying the gradient strength, copolymer composition, and molecular weight, and elucidating their impact on blend morphology, thermal stability, and device performance. We also plan to apply the gradient copolymer strategy to other polymer/fullerene-based devices where the performance is not as sensitive to the phase purity of the polymer as P3HT. In addition, extending the principles gleaned herein to donor–acceptor low band-gap copolymers with optimized HOMO/LUMO levels will advance our understanding of the complex interplay between mixing and de-mixing, with the attendant effects on performance, in bulk heterojunction devices.

## Acknowledgements

## Notes and references

1 For recent reviews, see: (a) M. C. Scharber and N. S. Sariciftci, *Prog. Polym. Sci.*, 2013, **38**, 1929–1940; (b) S. B. Darling and F. Q. You, *RSC Adv.*, 2013, **3**, 17633–17648.

2 For a comprehensive review, see: M. T. Dang, L. Hirsch and G. Wantz, *Adv. Mater.*, 2011, **23**, 3597–3602.

3 For reviews, see: (a) F. Liu, Y. Gu, J. W. Jung, W. H. Jo and T. P. Russell, *J. Polym. Sci., Part B: Polym. Phys.*, 2012, **50**, 1018–1044; (b) W. Chen, M. P. Nikiforov and S. B. Darling, *Energy Environ. Sci.*, 2012, **5**, 8045–8074; (c) C. J. Brabec, M. Heeney, I. McCullouch and J. Nelson, *Chem. Soc. Rev.*, 2011, **40**, 1185–1199; (d) M. A. Brady, G. M. Su and M. L. Chabinyc, *Soft Matter*, 2011, **7**, 11065–11077; (e) J. Peet, A. J. Heeger and G. C. Bazan, *Acc. Chem. Res.*, 2009, **42**, 1700–1708; (f) X. Yang and J. Loos, *Macromolecules*, 2007, **40**, 1353–1362.

4 For recent examples, see: (a) E. Verploegen, C. E. Miller, K. Schmidt, Z. N. Bao and M. F. Toney, *Chem. Mater.*, 2012, **24**, 3923–3931; (b) T. A. Bull, L. S. C. Pingree, S. A. Jenekhe, D. S. Ginger and C. K. Luscombe, *ACS Nano*, 2009, **3**, 627–636; (c) M. Campoy-Quiles, T. Ferenczi, T. Agostinelli, P. G. Etchegoin, Y. Kim, T. D. Anthopoulos, P. N. Stavrinou, D. D. C. Bradley and J. Nelson, *Nat. Mater.*, 2008, **7**, 158–164.

This journal is © The Royal Society of Chemistry 2014

*J. Mater. Chem. C*, 2014, **2**, 3401–3406 | **3405**

5 F. S. Bates, *Science*, 1991, **251**, 898–905.

6 (*a*) J. Kim, R. W. Sandoval, C. M. Dettmer, S. T. Nguyen and J. M. Torkelson, *Polymer*, 2008, **49**, 2686–2697; (*b*) Y. Tao, J. Kim and J. M. Torkelson, *Polymer*, 2006, **47**, 6773–6781; (*c*) J. Kim, H. Zhou, S. T. Nguyen and J. M. Torkelson, *Polymer*, 2006, **47**, 5799–5809; (*d*) J. Kim, M. K. Gray, H. Zhou, S. T. Nguyen and J. M. Torkelson, *Macromolecules*, 2005, **38**, 1037–1040; (*e*) Y. Tao, A. H. Lebovitz and J. M. Torkelson, *Polymer*, 2005, **46**, 4753–4761.

7 See also: (*a*) D. Sun and H. Guo, *J. Phys. Chem. B*, 2012, **116**, 9512–9522; (*b*) R. Malik, C. K. Hall and J. Genzer, *Soft Matter*, 2011, **7**, 10620–10630; (*c*) U. Beginn, *Colloid Polym. Sci.*, 2008, **286**, 1465–1474.

8 For a recent review, see: S. H. Anastasiadis, *Adv. Polym. Sci.*, 2011, **238**, 179–269.

9 (*a*) R. W. Sandoval, D. E. Williams, J. Kim, C. B. Roth and J. M. Torkelson, *J. Polym. Sci., Part B: Polym. Phys.*, 2008, **46**, 2672–2682; (*b*) C. L. H. Wong, J. Kim, C. B. Roth and J. M. Torkelson, *Macromolecules*, 2007, **40**, 5631–5633.

10 For examples of other additives used in stabilizing polymer/fullerene blends, see: (i) block copolymers: (*a*) M. Q. Chen, M. H. Li, H. T. Wang, S. X. Qu, X. M. Zhao, L. X. Xie and S. F. Yang, *Polym. Chem.*, 2013, **4**, 550–557; (*b*) C. Yang, J. K. Lee, A. J. Heeger and F. Wudl, *J. Mater. Chem.*, 2009, **19**, 5416–5423; (ii) alternating copolymers: (*c*) J. M. Lobez, T. L. Andrew, V. Bulovic and T. M. Swager, *ACS Nano*, 2012, **6**, 3044–3056; (iii) small molecules: (*d*) J. B. Kim, K. Allen, S. J. Oh, S. Lee, M. F. Toney, Y. S. Kim, C. R. Kagan, C. Nuckolls and Y. L. Loo, *Chem. Mater.*, 2010, **22**, 5762–5773; (*e*) J. K. Lee, W. L. Ma, C. J. Brabec, J. Yuen, J. S. Moon, J. Y. Kim, K. Lee, G. C. Bazan and A. J. Heeger, *J. Am. Chem. Soc.*, 2008, **130**, 3619–3623.

11 For examples of alternative approaches to stabilizing polymer/fullerene blends, see: (i) cross-linking polymers: (*a*) F. Ouhib, M. Tomassetti, J. Manca, F. Piersimoni, D. Spoltore, S. Bertho, H. Moons, R. Lazzaroni, S. Desbief, C. Jerome and C. Detrembleur, *Macromolecules*, 2013, **46**, 785–795; (*b*) C. Y. Nam, Y. Qin, Y. S. Park, H. Hlaing, X. H. Lu, B. M. Ocko, C. T. Black and R. B. Grubbs, *Macromolecules*, 2012, **45**, 2338–2347; (ii) cross-linking or polymerizing fullerene derivatives: (*c*) Y. J. Cheng, C. H. Hsieh, P. J. Li and C. S. Hsu, *Adv. Funct. Mater.*, 2011, **21**, 1723–1732; (*d*) V. A. Kostyanovsky, D. K. Susarova, A. S. Peregudov and P. A. Troshin, *Thin Solid Films*, 2011, **519**, 4119–4122.

12 For recent reviews, see: (*a*) Z. J. Bryan and A. J. McNeil, *Macromolecules*, 2013, **46**, 8395–8405; (*b*) T. Yokozawa, Y. Nanashima and Y. Ohta, *ACS Macro Lett.*, 2012, **1**, 862–866; (*c*) A. J. McNeil and E. L. Lanni, *New Conjugated Polymers and Synthetic Methods in Synthesis of Polymers*, ed. D.A. Schlüter, C. J.Hawker and J. Sakamoto, Wiley-VCH, Germany, 2012, vol. 1, pp. 475–486; (*d*) A. Kiriy, V. Senkovskyy and M. Sommer, *Macromol. Rapid Commun.*, 2011, **32**, 1503–1517.

13 For examples of other gradient copolymers synthesized *via* CTP, see: (*a*) E. F. Palermo, H. L. van der Laan and A. J. McNeil, *Polym. Chem.*, 2013, **4**, 4606–4611; (*b*) E. F. Palermo and A. J. McNeil, *Macromolecules*, 2012, **45**, 5948–5955; (*c*) J. R. Locke and A. J. McNeil, *Macromolecules*, 2010, **43**, 8709–8710.

14 L. Zhai, R. L. Pilston, K. L. Zaiger, K. K. Stokes and R. D. McCullough, *Macromolecules*, 2003, **36**, 61–64.

15 S. Miyanishi, Y. Zhang, K. Hashimoto and K. Tajima, *Macromolecules*, 2012, **45**, 6424–6437.

16 The longer retention time (and thus lower apparent molecular weight) for the fullerene-functionalized polymer is likely due to an increased affinity between the fullerene and the stationary phase. For reference, see: A. Kraus and K. Mullen, *Macromolecules*, 1999, **32**, 4214–4219.

17 A. J. Pearson, T. Wang, R. A. L. Jones, D. G. Lidzey, P. A. Staniec, P. E. Hopkinson and A. M. Donald, *Macromolecules*, 2012, **45**, 1499–1508.

18 (*a*) D. E. Motaung, G. F. Malgas and C. J. Arendse, *J. Mater. Sci.*, 2010, **45**, 3276–3283; (*b*) M. Theander, A. Yartsev, D. Zigmantas, V. Sundstrom, W. Mammo, M. R. Andersson and O. Inganas, *Phys. Rev. B: Condens. Matter Mater. Phys.*, 2000, **61**, 12957–12963; (*c*) N. S. Sariciftci, L. Smilowitz, A. J. Heeger and F. Wudl, *Science*, 1992, **258**, 1474–1476.

19 (*a*) A. Wagenpfahl, D. Rauh, M. Binder, C. Deibel and V. Dyakonov, *Phys. Rev. B: Condens. Matter Mater. Phys.*, 2010, **82**, 115306; (*b*) J. C. Wang, X. C. Ren, S. Q. Shi, C. W. Leung and P. K. L. Chan, *Org. Electron.*, 2011, **12**, 880–885; (*c*) B. Ecker, H. J. Egelhaaf, R. Steim, J. Parisi and E. von Hauff, *J. Phys. Chem. C*, 2012, **116**, 16333–16337; (*d*) J. Wagner, M. Gruber, A. Wilke, Y. Tanaka, K. Topczak, A. Steindamm, U. Hormann, A. Opitz, Y. Nakayama, H. Ishii, J. Pflaum, N. Koch and W. Brutting, *J. Appl. Phys.*, 2012, **111**, 054509; (*e*) W. Tress and O. Inganas, *Sol. Energy Mater. Sol. Cells*, 2013, **117**, 599–603; (*f*) B. Y. Finck and B. J. Schwartz, *Appl. Phys. Lett.*, 2013, **103**, 053306.

20 (*a*) C. Groves, *Energy Environ. Sci.*, 2013, **6**, 3202–3217; (*b*) B. P. Lyons, N. Clarke and C. Groves, *Energy Environ. Sci.*, 2012, **5**, 7657–7663; (*c*) H. P. Yan, S. Swaraj, C. Wang, I. Hwang, N. C. Greenham, C. Groves, H. Ade and C. R. McNeill, *Adv. Funct. Mater.*, 2010, **20**, 4329–4337.

21 (*a*) H. C. Liao, C. C. Ho, C. Y. Chang, M. H. Jao, S. B. Darling and W. F. Su, *Mater. Today*, 2013, **16**, 326–336; (*b*) A. Pivrikas, H. Neugebauer and N. S. Sariciftci, *Sol. Energy*, 2011, **85**, 1226–1237.

22 For a recent review, see: A. Yassara, L. Miozzoa, R. Girondaa and G. Horowitza, *Prog. Polym. Sci.*, 2013, **38**, 791–844.

23 (*a*) J. U. Lee, J. W. Jung, T. Emrick, T. P. Russell and W. H. Jo, *Nanotechnology*, 2010, **21**, 105201; (*b*) V. Gernigon, P. Leveque, C. Brochon, J.-N. Audinot, N. Leclerc, R. Bechara, F. Richard, T. Heiser and G. Hadziioannou, *Eur. Phys. J.: Appl. Phys.*, 2011, **56**, 34107; (*c*) K. Sivula, Z. T. Ball, N. Watanabe and J. M. J. Fréchet, *Adv. Mater.*, 2006, **18**, 206–210.